

RESEARCH ARTICLE

Modulated T-complex protein 1 ζ and peptidyl-prolyl *cis-trans* isomerase B are two novel indicators for evaluating lymph node metastasis in colorectal cancer: Evidence from proteomics and bioinformatics

Fei Yue¹, Li-Shun Wang², Li Xia², Xiao-Ling Wang², Bo Feng¹, Ai-Guo Lu¹, Guo-Qiang Chen² and Min-Hua Zheng^{1*}

¹Department of General Surgery, Ruijin Hospital, Shanghai Jiao Tong University School of Medicine, Shanghai, P. R. China

²Department of Pathophysiology, Key Laboratory of Cell Differentiation and Apoptosis of Chinese Ministry of Education, Shanghai Jiao Tong University School of Medicine, Shanghai, P. R. China

Lymph node metastasis (LNM) is an important indicator for systematic therapy, which could increase the survival of colorectal cancer (CRC) patients. However, effective clinical evaluation for LNM is still absent to date. In this study, protein expression profiles of CRC tissues were compared between patients with and without LNM. Based on average expression level, 12 proteins were found to be differentially expressed in the CRC tissues with LNM, whose discrimination reliability was confirmed by PCA. With stepwise linear discriminant analysis, T-complex protein 1 ζ subunit and peptidyl-prolyl *cis-trans* isomerase B (PPIB) were identified as two main contributors for separating CRC tissues with positive LNM from those negative ones in both original-grouped and cross-validated-grouped cases, which was also supported in subsequent linear support vector machine analysis. In addition, the expression alterations of the two proteins were verified by Western blot and immunohistochemistry. Functional studies also confirmed the role of PPIB in migration and invasion of cancer cells. Taken together, the down-regulated T-complex protein 1 ζ subunit and up-regulated PPIB were identified as two promising indicators for the clinical evaluation of LNM in CRC patients.

Received: February 26, 2009

Revised: July 5, 2009

Accepted: July 11, 2009



Keywords:

Bioinformatics / Colorectal cancer / Lymph node metastasis / Peptidyl-prolyl *cis-trans* isomerase B / T-complex protein 1 ζ subunit

1 Introduction

Colorectal cancer (CRC) is the third most common malignancy and represents one of the primary causes of cancer deaths in

Europe and the USA [1]. Many Asian countries, including China, Japan, South Korea, and Singapore, have been experiencing an increase of two to four times in the incidence of CRC during the past few decades [2]. As estimated [1], there are approximately 1 000 000 new cases of CRC and 500 000 deaths associated with CRC each year in the world. There is evidence that early diagnosis, before symptoms appear, reduces disease mortality and incidence of CRC patients [3]. Therefore, to explore biomarkers for early detection of CRC is useful and urgent for the clinical need. With the common applications of the developing genomic and proteomic

Correspondence: Dr. Guo-Qiang Chen, No. 280, Chong-Qing South Road, Shanghai 200025, P. R. China

E-mail: chengq@shsmu.edu.cn

Fax: +86-21-64154900

Abbreviations: CRC, colorectal cancer; LDA, linear discriminant analysis; LNM, lymph node metastasis; LN⁻, negative LNM; LN⁺, positive LNM; NC, negative control; PC, principal component; PPIase, peptidyl-prolyl *cis-trans* isomerase; PPIB, peptidyl-prolyl *cis-trans* isomerase B; SVM, support vector machine; TCPZ, T-complex protein 1 ζ subunit; TCP1, T-complex protein 1

*Additional corresponding author: Dr. Min-Hua Zheng

E-mail: zmhtiger@yeah.net

techniques such as DNA microarray, 2-DE and MS, a series of potential biomarkers in cells, tissues, and bodily fluids that will aid the diagnosis of CRC were recently uncovered and are currently being used in clinical settings or may be used in the future, as widely reviewed by Lee's group [4].

Although there is a controversy regarding the association between diagnostic or therapeutic delay and survival when the CRC patients already have symptoms [5, 6]. On the other hand, lymph node metastasis (LNM) is believed to be one of the strong negative prognostic factors for CRC patients [7]. Accordingly, the evaluation of LNM is also essential for the clinicians to determine proper pre-operative neo-adjuvant therapies as well as post-operative adjuvant therapies, which can significantly improve the survival of CRC patients with positive LNM (LN⁺) [8]. The computerized tomography scan is applied to pre-operative clinical staging of CRC, but it is intrinsically limited for nodal metastasis staging due to the existence of normal-sized lymph nodes with metastasis and enlarged benign nodes [9]. In fact, the evaluation of LNM is still mainly dependent on post-operative pathological examination of resected lymph nodes, which risks the loss of metastasized nodes [10]. Therefore, it is also of great significance to explore novel indicators for the detection of LNM in CRC [11]. More recently, Shen's group reported that the increased HSP-27, glutathione *S*-transferase, and annexin II proteins but the decreased liver-fatty acid-binding protein suggest a significantly elevated incidence of LNM in CRC through 2-DE analysis, followed by immunohistochemistry staining in paraffin-embedded CRC samples [12]. Additionally, the conditioned media of CRC cell lines-based secretome analysis showed that collapsin response mediator protein-2-positive rate was significantly increased in CRC at earlier stage and with LNM [13]. Based on the data obtained from comparative proteomic and bioinformatic analyses on 12 CRC tissues, Western blot, immunohistochemistry on tissue microarray from 83 consecutive CRC patients, as well as wound healing assay and cell invasion assay on SW480 cells with reduced PPIB expression, here we show that the down-regulation of T-complex protein 1 ζ subunit (TCPZ) and up-regulation of peptidyl-prolyl *cis-trans* isomerase B (PPIB) were commonly presented in CRC tissues with LNM, suggesting that they might be potentially valuable for clinical evaluation of LNM in CRC patients.

2 Materials and methods

2.1 Patients and tissue preparation

For proteomic and bioinformatic analyses, 12 cases of moderately differentiated colorectal adenocarcinoma (four males and eight females, aging 50–80 years; for details see Supporting Information Table S1), who underwent surgical resections of primary sporadic CRC, were randomly collected from the Department of General Surgery, Ruijin Hospital, Shanghai Jiao Tong University School of Medicine. According to the latest TNM staging criteria [14], they

were divided into two groups of negative LNM (LN⁻) and LN⁺ with six cases in each group. There was no LNM found in the subjects of the LN⁻ group. Fresh CRC tissues and paired non-cancer adjacent tissues were obtained immediately after the surgery, snap-frozen immediately in liquid nitrogen, and then stored at -80°C before analysis.

For tissue microarray, 83 paraffin-embedded primary CRC tissues (48 males and 35 females, aging 59 ± 11.5 years, TNM staging from I–IV, Table 1) were collected consecutively from patients who received radical resections at Ruijin Hospital in 2007. All patients enrolled in this study received neither chemotherapy nor radiotherapy before the surgery. The tissue microarray was constructed with an ATA-27 automated arrayer (Beecher Instruments, WI, USA). Sections of $4\ \mu\text{m}$ were deparaffinized with xylene and ethanol for further immunohistochemistry staining. The study was approved by the Research Ethics Committee of Shanghai Jiao Tong University School of Medicine. The written consents were obtained from all patients.

2.2 Proteomic analysis and protein identification

Briefly, frozen tissues were pulverized and mixed with 10% trichloroacetic acid in chilled acetone containing 20 mM DTT overnight to get complete protein precipitation. The pellets were then resuspended with lysis buffer containing 7 M urea, 2 M thiourea, 4% CHAPS, 40 mM Tris, and separated with 2-DE. For the first dimension, the proteins were loaded on to 17 cm IPG strips with a non-linear range of pH 3–10 (Bio-Rad, CA, USA) for the separation according to their *pI*. The focusing was started at 200 V for 30 min, 500 V for 30 min, 1000 V for 1 h followed by linearly ramping up to 10 000 V for 2 h and then kept at 10 000 V until 60 000 Vh were reached. Then the strips were transferred to the second dimension 12% SDS-PAGE for the separation according to the molecular weight. The vertical electrophoresis was first performed at a constant current of 16 mA *per gel* for 30 min, followed by a constant 24 mA *per gel* until the bromophenol blue dye reached the bottom of the gels. The separated proteins were visualized with silver staining. The images of the stained gels were acquired with GS-800-calibrated densitometer (Bio-Rad). The raw density of protein spots was normalized to the total density in gel image, and the normalized spot density was analyzed with PDQuest 7.20 software (Bio-Rad).

The protein identification was carried out with MALDI-TOF/TOF mass spectrometer 4700 Proteomics Analyzer (Applied Biosystems, CA, USA). Briefly, the spots of interest were excised, destained, and followed by digestion with sequencing grade-modified porcine trypsin (Promega, WI, USA). C₁₈-ZipTip (Millipore, MA, USA) was used to desalt and extract the digested peptides according to the manufacturer's instruction. The desalted and concentrated peptides were lyophilized and suspended in $2\ \mu\text{L}$ matrix solution containing $10\ \mu\text{g}/\mu\text{L}$ CHCA in 50% ACN and 0.1%

Table 1. Data of patients for microarray and associations of TCPZ and PPIB expression with clinicopathological factors in CRC

Factor	TCPZ				PPIB			
	Negative ^{a)}	Positive ^{a)}	Rate (%)	<i>p</i> ^{b)}	Negative ^{a)}	Positive ^{a)}	Rate (%)	<i>p</i> ^{b)}
Age								
<60	13	28	68.29		13	28	68.29	
≥60	15	27	64.29	0.699	18	24	57.14	0.294
Gender								
Female	11	24	68.57		11	24	68.57	
Male	17	31	64.58	0.704	20	28	58.33	0.341
Location								
Colon	22	43	66.15		23	42	64.62	
Rectum	6	12	66.67	0.968	8	10	55.56	0.482
Local invasion								
T1-T2	4	12	75.00		6	10	62.50	
T3-T4	24	43	64.18	0.411 ^{c)}	25	42	62.69	0.989
LNM								
Negative	10	36	78.26		25	21	45.65	
Positive	18	19	51.35	0.010	6	31	83.78	0.000
Remote metastasis								
Negative	24	50	67.57		29	45	60.81	
Positive	4	5	55.56	0.478 ^{c)}	2	7	77.78	0.473 ^{c)}

a) Negative and positive means negative and positive expression of proteins as indicated.

b) *p*-Value between different groups in terms of factors as indicated.

c) Fisher's exact test.

TFA. An aliquot of 0.7 μL was spotted onto the MALDI target. Prior to real sample acquisition, six calibrated spots were used for signal and parameter optimization. The PMF was obtained in the mass range between 800 and 4000 Da with 2000 laser shots. To obtain the spectra with the mass accuracy of less than 50 ppm, trypsin autocatalytic peaks were used for the internal calibration.

The proteins of interest were analyzed and identified by searching the Swiss-Prot protein database using the MASCOT search engine (Matrix Science, MA, USA) integrated in the Global Protein Server Workstation. The mass tolerance was limited to 50 ppm. The results from both PMF and MS/MS spectra were accepted as a positive identification when the score confidence was higher than 95% by the Global Protein Server Workstation.

2.3 Western blot

Twenty microgram protein extracts of 12 CRC tissues were separated with 12% SDS-PAGE, and transferred to nitrocellulose membranes (Axygen, CA, USA). Membranes were blotted by goat anti-TCPZ antibody (Santa Cruz, CA, USA) or rabbit anti-PPIB antibody (ProteinTech, IL, IL), followed by HRP-conjugated anti-goat IgG antibody (Dako, Glostrup, Denmark) or anti-rabbit IgG antibody (Cell Signaling, MA, IL). HRP-conjugated mouse anti-GAPDH antibody (Kang-Chen, Shanghai, China) was used as the loading control. The proteins were detected with an ECL detection system (Pierce, IL, USA), and developed onto Kodak X-ray films. The images on the films were acquired with GS-800-cal-

ibrated densitometer and quantified with QuantityOne 4.63 software (Bio-Rad, CA, USA).

2.4 Immunohistochemistry on tissue microarray

Immunohistochemical staining was carried out using the same primary antibodies applied in Western blot on tissue microarrays containing 83 CRC tissues according to the manufacturers' instructions. Briefly, after blocking endogenous peroxidase activity, tissue microarrays were incubated with anti-TCPZ antibody or anti-PPIB antibody overnight, then incubated with HRP polymer-conjugated anti-goat IgG kit (Zhongshan, Beijing, China) or EnVision anti-mouse/rabbit IgG kit (Dako), visualized with diaminobenzidine, and counterstained with hematoxylin. The immunostaining was scored in a semi-quantitative scale: positive staining cells with less than 25, 25–50, 50–75% and more than 75% were scored as 1+, 2+, 3+, and 4+, respectively [15]. Tissue dots with scores of 3+ or 4+ were designated as "positive", whereas the dots with scores of 1+ or 2+ were designated as "negative". The staining results were scored independently by two pathologists. The results from the two pathologists were compared, and the samples in which there were discrepancies were re-evaluated by them together to reach a consensus.

2.5 Cell culture and RNA interference of PPIB

CRC cell line SW480 were cultured in RPMI-1640 (Sigma-Aldrich, MI, USA) supplemented with 10% FBS (Gibco, MD,

USA) and incubated in 5% CO₂/95% air in a humidified atmosphere at 37°C. In order to generate SW480 cells with reduced PPIB expression, the target sequence for PPIB mRNA silencing (siPPIB: 5'-CGC AAC ATG AAG GTG CTC C-3') was designed with online software *siRNA Target Finder* (Ambion, TX, USA) http://www.ambion.com/techlib/misc/siRNA_finder.html. According to the manufacturer's instructions, the siPPIB sequence was synthesized and inserted into the pSilencer 3.1-H1 neo vector (Ambion). The siPPIB-containing vectors and the negative control (NC) vectors were transfected into SW480 using Lipofectamine 2000 (Invitrogen, CA, USA). Twenty-four hours after transfection, 1 mg/mL G418 (Calbiochem, NJ, USA) was added into the culture medium for the selection of stably transfected cells. The SW480 cells with siPPIB and NC sequences were designated as SW480-siPPIB and SW480-NC.

2.6 Wound-healing assay

SW480-siPPIB and SW480-NC cells were seeded in a Matrigel (Becton Dickinson, MA, USA)-coated 6-well plate to form a monolayer. Then, a wound strip was made with a sterile pipette tip in the middle of the plate. Afterward, cells were rinsed and cultured in serum-free RPMI-1640 medium, images were immediately acquired by Olympus BX51 microscope, and the wound distance as the basis width was measured with NIS-Elements software (Nikon Instruments, NY, USA). After 24 h incubation, cells were washed three times with PBS. Migration of cells into the wound was recorded and the wound closure was determined as the width migrated after 24 h relative to the basis width. This assay were carried out in triplicate and repeated thrice.

2.7 Cell invasion assay

The BioCoat Matrigel Invasion Chambers (Becton Dickinson) was applied for the assessment of cell invasiveness of SW480-siPPIB and SW480-NC. Briefly, cells were harvested, resuspended in serum-free RPMI-1640, added in to the upper compartment (2×10^5 per well) of pre-hydrated Matrigel-coated invasion chambers. The lower compartment was filled with RPMI-1640 containing 10% FBS. After incubation for 24 h, the Matrigel and non-invading cells in the upper compartment were scrubbed with moistened cotton swabs. Then, the membranes immersed in the lower compartment were fixed by methanol and stained with Wright-Giemsa stain. The numbers of cells migrated through the Matrigel-coated membrane were calculated using microscope. The assay was carried out independently for three times.

2.8 Statistical and bioinformatic analyses

The statistical analyses were performed with SPSS 13.0 (SPSS, IL, USA). The protein expression differences in 2-DE

and Western blot were determined with Student's *t*-test. PCA was applied to validate the reliability of identified altered proteins by the discrimination of LN⁻ and LN⁺ CRC [16]. Stepwise linear discriminant analysis (LDA) is used for variable selection and sample classification, which can find proteins with the most significant contribution to the sample discrimination. During the stepwise introduction of variables, the *p*-values of entry and removal were set as 0.05 and 0.10, respectively. Linear support vector machine (SVM) analysis was carried out with Matlab 7.0 software (The MathWorks, MA, USA) for further validation of the data derived from small sample population [17]. The associations of protein expression with clinical pathological factors were determined by Chi-square test. It was considered as statistically significant when $p < 0.05$.

3 Results

3.1 Identification of proteins with specific differential expression in LN⁺ CRC

To reveal the most significantly changed proteins in the CRC tissue with LNM, cancer tissues were divided into LN⁻ and LN⁺ groups, which were extracted separately and pooled. Then the pooled protein extracts were separated with 2-DE in triplicate. Totally, 1930 ± 265 spots were detected and the overall protein expression profile with *pI* 3–10 and molecular weight between 10 and 100 kDa had a good reproducibility (Fig. 1A). According to the densities of spots normalized to the total density on gel, 15 protein spots with the mean change fold of higher than 1.5-fold were found, among which eight were up-regulated and seven were down-regulated. Furthermore, the analyses of the protein expression profiles of paired non-cancer adjacent tissues in the LN⁻ and LN⁺ groups showed that densities of 14 spots presented no change in non-cancer adjacent tissues (Fig. 1B), except that the Spot 2 showing the similar alteration in non-cancer adjacent tissue and cancer tissues (Fig. 1C). Furthermore, these 14 spots were tested individually in all samples. The results showed that the expression alterations of the spots 6 and 7 were attributed to extreme changes in individual samples. Therefore, the remaining 12 differentially expressed proteins that still had consistent alterations in individual samples (Figs. 2A–D) were identified with PMF and MS/MS (Table 2 and Figs. 2E and F).

3.2 PCA analysis on proteins with specific differential expressions in LN⁺ CRC

The normalized protein densities obtained from individual sample gels were first validated with PCA, as described by Rodriguez-Pineiro *et al.* [16]. With the first three principal components (PCs), the 12 CRC patients formed two clusters in the resulting 3-D plot and most of them were correctly

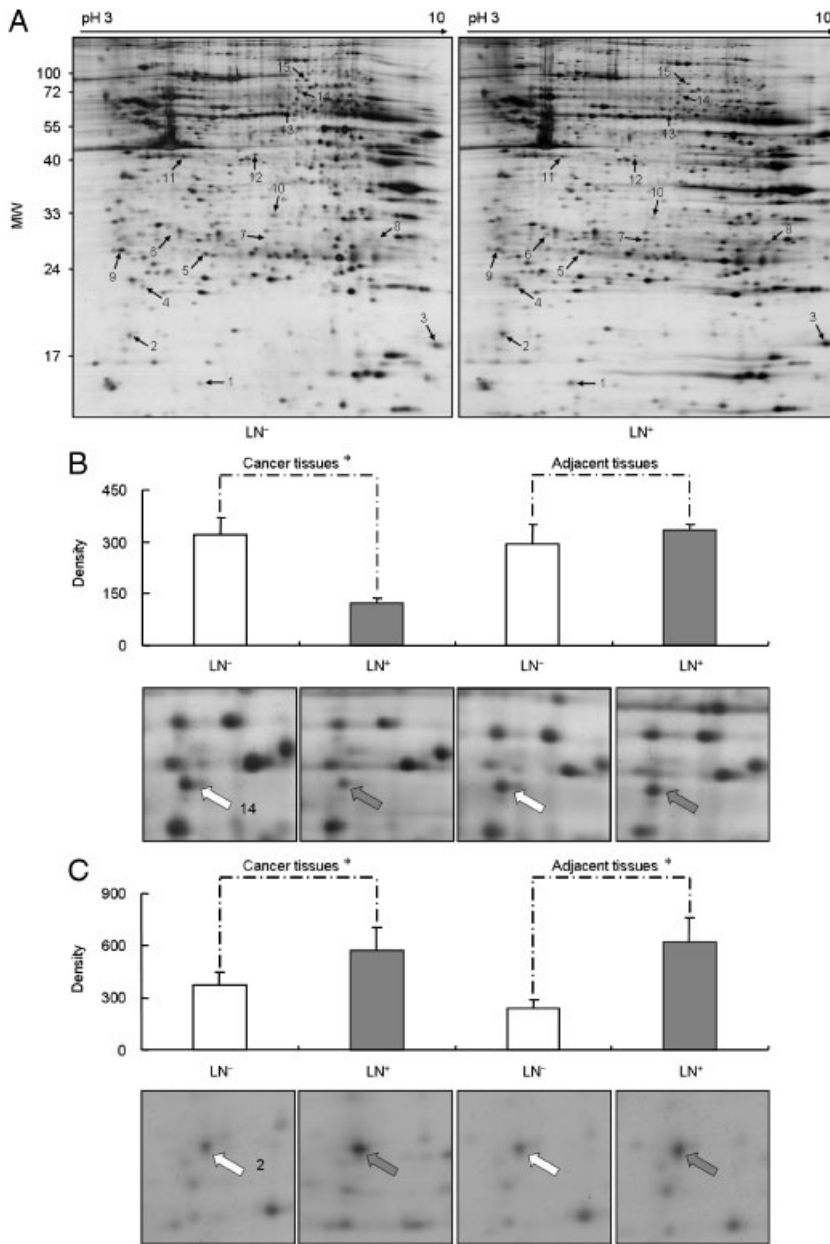


Figure 1. Differentially expressed protein spots between CRC tissues with and without LNM. (A) Pooled protein extracts (200 μg) of cancer tissues from LN⁻ and LN⁺ (six cases each) were respectively separated with 2-DE. The experiments were repeated in triplicate and a pair of representative 2-DE images is shown, in which differentially expressed spots pointed by arrows are labeled with serial numbers. (B) A representative protein spot (Spot 14) which represents altered expression only in CRC tissues with LNM. (C) Spot 2 shows similar alteration in non-cancer adjacent tissue and cancer tissues with or without LNM. Their densities are shown in the top. The asterisk represents $p < 0.05$ between two groups linked by line.

clustered into LN⁻ and LN⁺ groups (Fig. 3A). In the 2-D plot with only PC1 and PC2, the samples could also be well separated. As shown in Fig. 3B, samples with a positive score in PC1 formed LN⁻ cluster, and those with a negative score formed LN⁺ cluster. Interestingly, there was one exception: sample #2 with LN⁻ got a negative score in PC1, but was clustered into the LN⁺ group. When tracing back to corresponding clinical information, it is found that this patient had a high pre-operative carcinoembryonic antigen level (36.14 ng/mL, Supporting Information Table S1), indicating a poor prognosis, which might be the reason for its drift into the LN⁺ group. These results validated the reliability of the 12 protein indicators in sample classification as proteomic signatures.

3.3 Two main contributors for the separation of CRC with and without LNM

In the next phase of analysis, stepwise LDA was applied to select the proteins with the highest power of discrimination. TCPZ and PPIB were identified as two main contributors which could correctly classifying 91.7% (11/12) of CRC samples with original grouping, and the accuracy was still maintained in the leave-one-out cross-validation (Table 3). We also applied linear SVM analysis, which is specially designed to deal with small sample population [18]. As shown in Fig. 3C, the 12 CRC patients were well classified into LN⁻ and LN⁺ according to the standardized TCPZ and PPIB densities from individual sample gels. In total, 83.3%

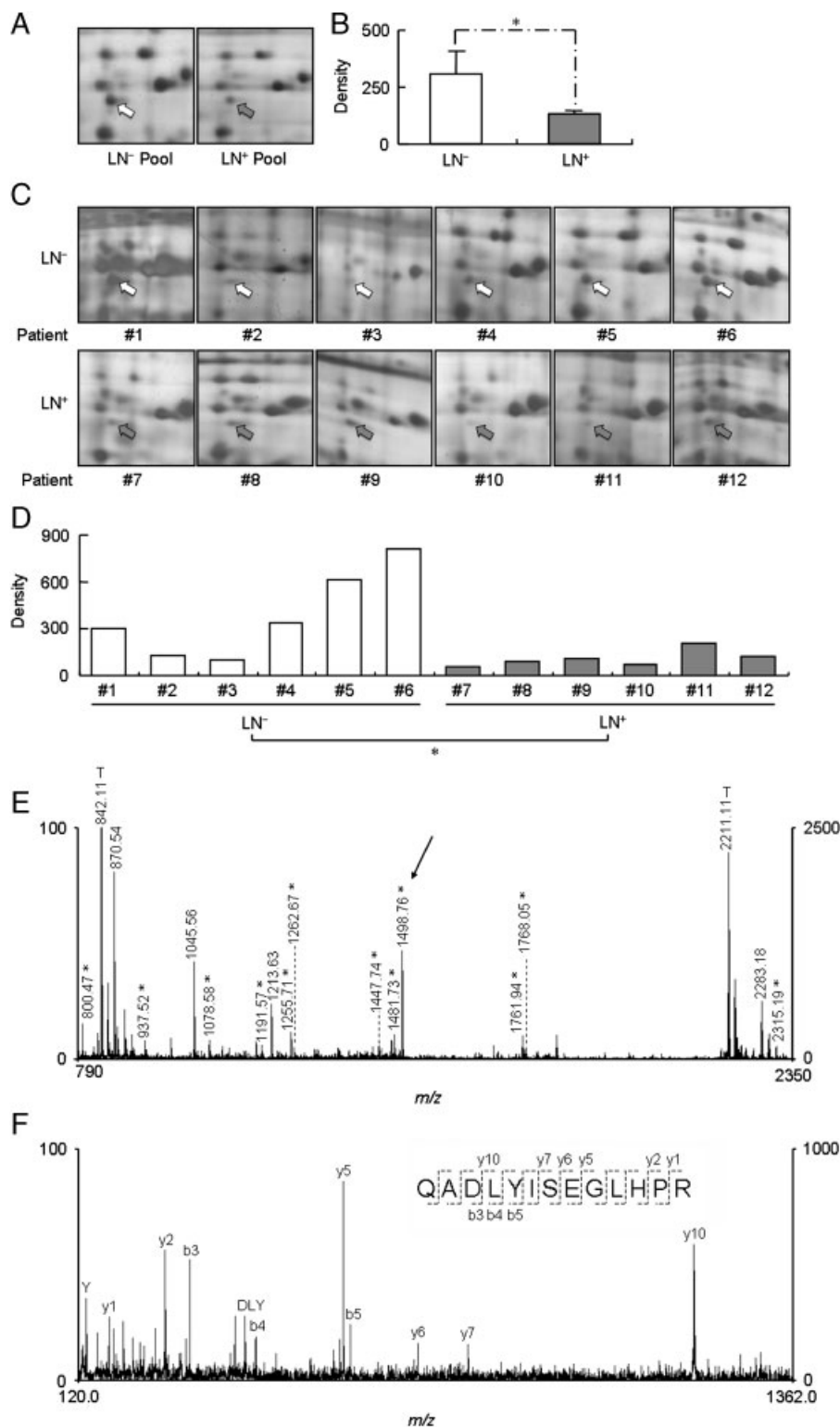


Figure 2. A representative spot (Spot 14) that demonstrated consistent and significant down-regulation in both pooled (A) and individual samples (C) in CRC tissues with LNM. Their densities are also shown in panels B and D, respectively. Spot 14 was then identified as TCPZ (E). Here, “T” indicates trypsin autocatalytic peptides for internal calibration and asterisks indicate peaks matching protein TCPZ. The matched peptides occupied 34% of the sequence coverage and obtained a score of 90. The arrow indicates the ion at m/z 1498.76 selected for MALDI-TOF/TOF MS/MS. (F) Fragmentation spectrum for ion 1498.76. The γ -ions and b -ions as well as internal fragment ions and immoium ions were denoted in the spectrum. The m/z 1498.76 is one of the abundant peaks selected for MS/MS acquisition. The identified sequence is QADLYISEGLHPR interpreted as γ -series and b -series ions, which were indicated in the top right corner. The asterisk represents $p < 0.05$.

(10/12) patients could still be correctly classified in the leave-one-out cross-validation. Both stepwise LDA and SVM analyses indicated that TCPZ and PPIB were two proteins that had major contributions to the discrimination of

LN^- and LN^+ CRC samples. Furthermore, Western blot analysis with the 12 cases of samples shown in Fig. 2C was performed for TCPZ (Fig. 4A) and PPIB (Fig. 4D), and the relative densities of their bands normalized to

Table 2. Differentially expressed proteins in CRC with LNM

Spot no.	Protein name	Acc. no.	Mean fold	MW (kDa) (expt./ theor.)	p/ (expt./ theor.)	ID method	Matched peptide	Coverage (%)	Score
1	Transthyretin	P02766	2.32	16/15.99	5.6/5.52	PMF	7	68	78
3	PPIB	P23284	1.69	19/22.79	9.5/9.33	PMF	19	59	138
4	Lactoylglutathione lyase	Q04760	1.74	21/20.80	5.0/5.25	PMF	7	35	60
5	HSP β -1	P04792	1.54	24/22.83	5.8/5.98	PMF	17	66	181
8	Galectin-3	P17931	1.67	27/26.10	8.2/8.61	PMF	11	35	109
9	Proteasome subunit α type 5	P28066	-1.69	27/26.57	4.5/4.74	MS/MS	1	5	68
10	Proteasome subunit α type 1	P25786	-1.60	33/36.14	6.8/8.16	PMF	14	46	77
11	Keratin, type I cytoskeletal 19	P08727	-1.56	41/44.08	5.5/5.04	PMF	35	75	344
12	Leukocyte elastase inhibitor	P30740	-2.68	42/42.83	6.4/5.90	PMF	17	48	150
13	Retinal dehydrogenase 1	P00352	-1.55	58/55.32	6.8/6.29	PMF	15	30	90
14	TCPZ	P40227	-3.34	65/58.31	6.9/6.25	PMF	16	34	90
15	WD-repeat protein 1	O75083	-1.71	73/66.71	7.0/6.18	PMF	21	42	163

Differentially expressed proteins identified in LN+ CRC tissues comparing to LN- ones. A software-aided spot intensity ratio (positive ratios stand for up-regulation and negative ratios stand for down-regulation in CRC tissues with LNM), as well as the experimental pI, and molecular weight are provided for each identified protein. Detailed information of identified peptide sequences are shown in Supporting Information Table S2. (Acc. no., accession number in Swiss-Prot; expt./theor., experimental versus theoretical).

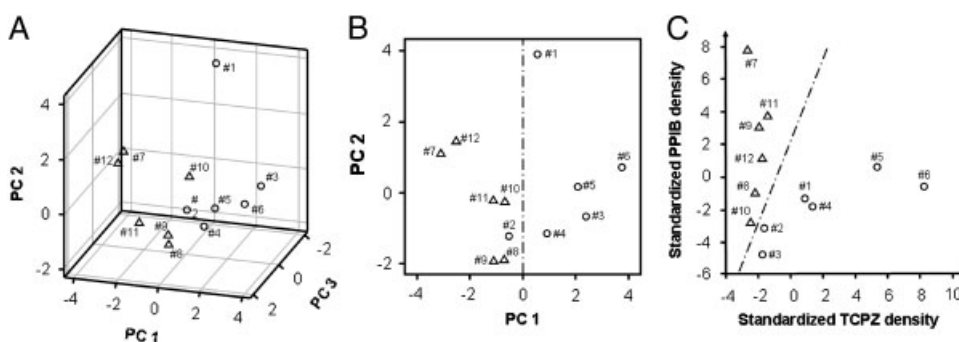


Figure 3. Bioinformatic analyses. (A) The 12 patients are well separated from one another in a 3-D scatter plot with the first three PCs as each axis especially in PC1. (B) The patients with positive scores in PC1 formed LN⁻ cluster and those with negative scores formed LN⁺ cluster. (C) With linear SVM analysis, TCPZ and PPIB were also verified to be capable of well classifying LN⁺ samples (Δ) from LN⁻ ones (\circ). # patients' serial numbers.

corresponding GAPDH were determined with Student's *t*-test. The results showed that TCPZ and PPIB presented statistically significant differences between CRC tissues with and without LNM (Figs. 4B and E).

3.4 Tissue microarray analysis for LNM evaluation in 83 cases of CRC patients

The above results suggested that TCPZ and PPIB might be promising indicators for LNM in CRC. To further validate, tissue microarray-based immunohistochemistry analysis on an additional 83 CRC tissues was performed. The result also demonstrated that TCPZ was down-regulated (Fig. 4C), whereas PPIB was up-regulated (Fig. 4F) in LN⁺ tissues. Statistical analysis on their scores showed that the alterations of the two proteins were significant between CRC tissues with and without LNM, whereas no significant

differences were found in other clinical factors, such as age, gender, location, local invasion, and remote metastasis (Table 1).

3.5 The suppression of PPIB expression inhibits migration and invasion of CRC cells

In order to further investigate whether the candidate proteins are involved in metastasis, the expression of PPIB was suppressed by RNA interference in SW480 cells. The protein expression of PPIB was drastically reduced in SW480-siPPIB but not in SW480-NC (Fig. 5A). The wound-healing assay demonstrated that the suppression of PPIB-inhibited cell migration, and the inhibition of closure rate are statistically significant (Figs. 5B and C). Moreover, in the cell invasion assay, remarkably less invaded cells were observed in SW480-siPPIB compared with that in

Table 3. Stepwise LDA

		Predicted group membership			Total
		Group	LN ⁻	LN ⁺	
Original	Count	LN ⁻	6	0	6
		LN ⁺	1	5	6
	%	LN ⁻	100.0	0.0	100.0
		LN ⁺	16.7	83.3	100.0
Cross-validated	Count	LN ⁻	6	0	6
		LN ⁺	1	5	6
	%	LN ⁻	100.0	0.0	100.0
		LN ⁺	16.7	83.3	100.0

After stepwise LDA, TCPZ, and PPIB are selected to build discriminant functions. Totally, 91.7% of both original-grouped and cross-validated-grouped cases are correctly classified.

SW480-NC, which is also statistically significant (Figs. 5D and E). Collectively, the above results indicate the involvement of up-regulated PPIB in the process of migration.

4 Discussion

In this study, we applied proteomic and bioinformatic strategies to identify potential biomarkers for evaluating LNM in CRC. To avoid those proteins present in only one or a few samples with extreme alteration appearing to be “significant”, a pool strategy was utilized to reduce their signal intensity in our study. Hence, a set of 12 consistently altered spots in both pooled samples and individual samples were found differentially expressed between LN⁻ and LN⁺ CRC tissues. Among these proteins, transthyretin, PPIB,

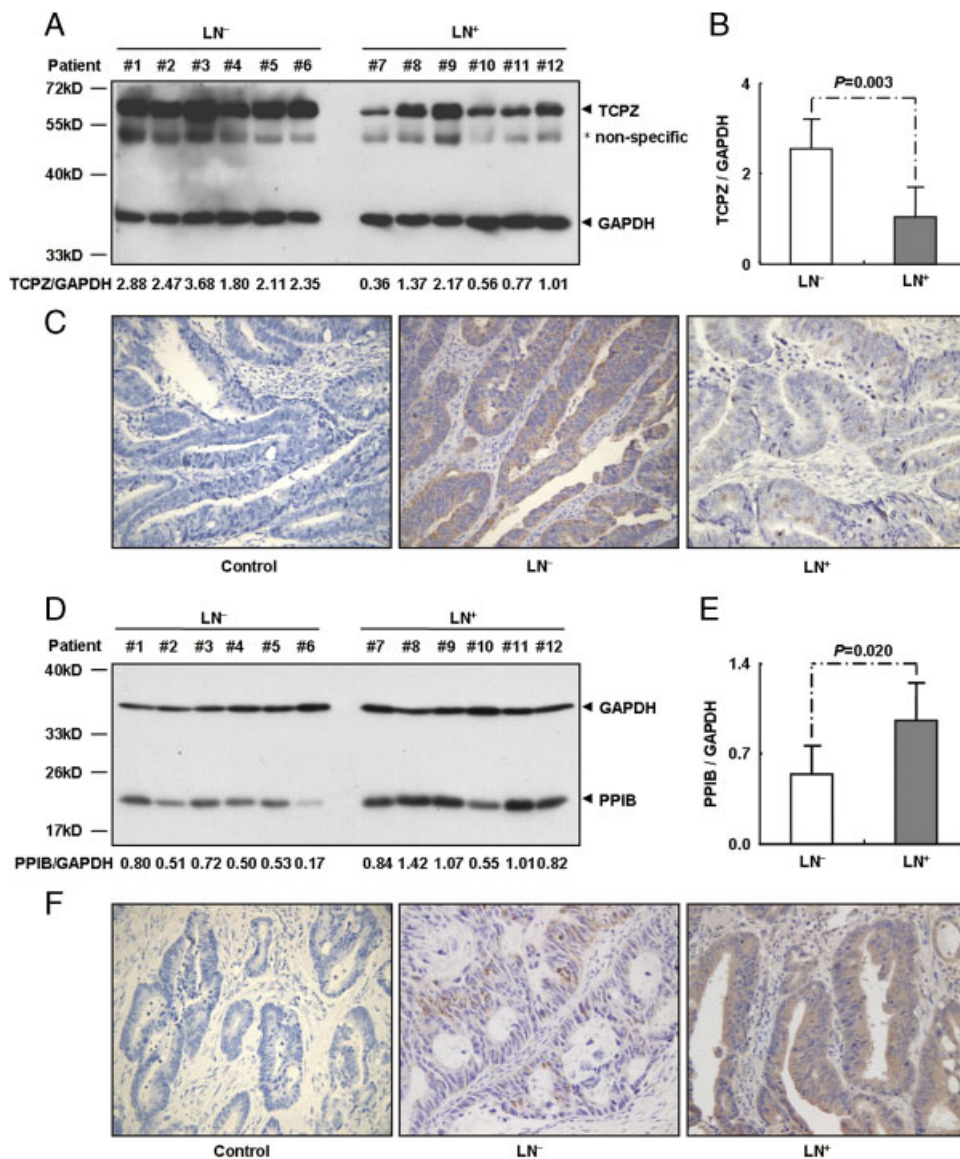


Figure 4. Validation of TCPZ and PPIB expression with Western blot and immunohistochemistry. Cancer tissues from 12 cases of CRC patients with or without LNM were blotted with anti-TCPZ antibody (A) or anti-PPIB antibody (D) and with GAPDH as loading control. The numbers on their bottom represent TCPZ/GAPDH (A) or PPIB/GAPDH (D) in corresponding patients. The ratios for TCPZ/GAPDH (B) and PPIB/GAPDH (E) from all CRC patients with and without LNM (six samples each) were expressed by the mean with bar as SD. Representative immunohistochemical staining for TCPZ (C) and PPIB (F) on 83 cases of LN⁻ and LN⁺ cancer tissue microarray. Tissues incubated with PBS instead of the primary antibodies serve as the control. Asterisk represents non-specific band.

lactoylglutathione lyase, and galectin-3 besides HSP β -1 (namely HSP27), reported previously [12], presented up-regulation, whereas down-regulation was observed in proteasome subunit α type 5, proteasome subunit α type 1, keratin type I cytoskeletal 19, leukocyte elastase inhibitor, retinal dehydrogenase 1, TCPZ, and WD-repeat protein 1.

Then the data set of protein densities was submitted to bioinformatic analyses. As is known, PCA defines the directions of maximum variance among samples and represents the samples in a multi-dimensional space constructed by the resulting dimensions [19]. According to the results of PCA, most of the samples were correctly clustered, which indicated the reliability of these differentially expressed proteins for the evaluation of LNM. As reported, more informative proteins do not mean more accurate in the multivariate analysis, and the most significant ones are better candidates as potential biomarkers [16]. Several research studies have well demonstrated the advantages of multivariate analysis on proteomic data sets to find the optimal signature for cancer classification [19–22]. Clinically, too many biomarkers are neither practical nor economical. For this reason, we applied stepwise LDA analysis to the density data set hoping to find out the main contributors from the identified 12 proteins. Intriguingly,

91.7% of both original-grouped and cross-validated-grouped cases could be correctly classified with only TCPZ and PPIB, indicating that TCPZ and PPIB were two main contributors which could effectively discriminate LN⁺ CRC from LN⁻ ones. SVM, whose algorithm is based on statistical learning theory, was implemented for validation of the selected two proteins, as it can solve the problem of machine learning with small sample population [17, 18]. Notably, after leave-one-out validation, the overall accuracy of correct classification is 83.3%, which further confirmed the reliability of TCPZ and PPIB in LNM evaluation. Results from both immunoblotting and immunochemistry assays were also consistent with the proteomic indications. Additionally, these results also supported that the bioinformatic analyses can be easily applied by the clinical researchers to their proteomic data for the selection of clinic-oriented indicators.

TCPZ is the ζ subunit of T-complex protein 1 (TCP1), the latter being also known as TCP1 ring complex or chaperonin-containing T-complex polypeptide 1. Previous reports showed increased expression of cytosolic TCP1/chaperonin-containing T-complex polypeptide 1 in human hepatocellular and colonic carcinoma [23, 24]; however, our proteomic study found that TCPZ is down-regulated in CRC tissues with LNM, which is also confirmed by immunoblotting and

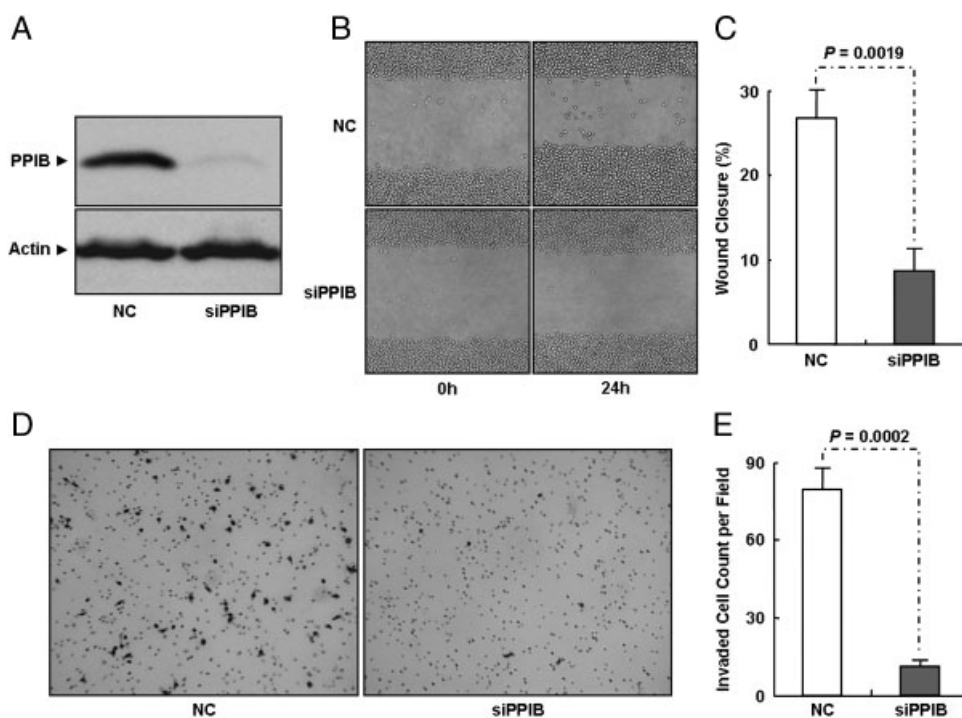


Figure 5. The suppression of PPIB expression inhibits migration and invasion of CRC cells. (A) The protein expression of PPIB was drastically suppressed in SW480 cells stably transfected with PPIB silencing sequence (SW480-siPPIB) but not in the NC vector with scramble sequence (SW480-NC). (B) The wound-healing assay showed that the migration of SW480-siPPIB cells was inhibited, as the wound closure rates were reduced significantly compared with that of SW480-NC cells. (D) In the cell invasion assay, remarkably less SW480-siPPIB cells invaded through the Matrigel-coated membrane compared with SW480-NC cells. (C and E) The values of both wound-healing assay and cell invasion assay were illustrated as means with bar as SD of three independent experiments, and *p*-values between two groups linked by lines are shown.

immunohistochemistry. As reported previously [25], TCP1 is a member of chaperonin family mediating the folding of newly synthesized proteins in an ATP-dependent manner. We speculated that the down-regulation of TCPZ may result in misfolding of a series of proteins which is specifically recognized by TCPZ, and those misfolded proteins may then play a role in LNM in CRC, although it remains to be further investigated whether and how the down-regulation of TCPZ is related to LNM in CRC.

PPIB, which obtains the activity of peptidyle-prolyl *cis-trans* isomerase (PPIase), acts as an acceleration factor in protein folding and assembly. Once the *cis-trans* isomerase activity is blocked, the maturation of collagen would be significantly delayed [26, 27]. Collagen is a main component of the extracellular matrix, which could hinder the metastasis of cancer cells. Besides, PPIB was also found to be capable of forming a transcriptional inducer, resulting in cell growth and proliferation, which would be abolished by the removal of PPIase activity of PPIB [28]. PPIB was found up-regulated in the CRC tissues with LNM according to our data. Functional experiments, including wound-healing assay and cell invasion assay, demonstrated that the suppression of PPIB inhibits migration and invasion of CRC cells, suggesting the substantial contribution of PPIB in LNM. A more recent study observed similar results in breast cancer cells [29]. Interestingly, up-regulation of other PPIase members was reported in diverse cancers previously, for instance, PPIA in hepatocellular cancer [30], lung cancer [31, 32], pancreatic [33, 34], and endometrial cancer [35]; PPID and FKBP52 in breast cancer [36]; PPIAL-4A in osteosarcoma [37]; and Pin1 in head and neck squamous cell carcinomas [38, 39]. Moreover, certain roles of PPIases played in cancers have been investigated. For example, PPIA has been identified as a target of hypoxia-inducible factor-1 α and protect cancer cells against apoptosis induced by cellular stress including hypoxia and cisplatin [40]; Pin1 inhibition in cancer cells would suppress cell proliferation, transformed phenotype and tumorigenesis, which makes Pin1 a promising anti-cancer molecular target [41]. Collectively, these literatures indicated that PPIase family members are of great importance for cancer patients as either potential biomarkers or therapeutic targets. However, more studies are required for detailed elucidation of PPIases' functions in tumors.

Taken together, our results proposed that TCPZ and PPIB have promising potentials for the evaluation of LNM in CRC. Extensive investigations on the detailed roles they play in LNM in CRC are still required. These discoveries would shed new clues for evaluating the clinicopathological characteristics of CRC with LNM and better understanding the mechanisms underlying CRC prognosis.

The authors thank Dr. Zhao-Wen Yan for her technical support by immunohistochemistry. This work was supported in part by grants from the Ministry of Science and Technology of P. R. China (2006AA02Z105), National Natural Science

Foundation of China (30500215; 30600261; 3087300), Shanghai Municipal Health Bureau (LJ06038), Shanghai Shengkang Hospital Development Center (SHDC12006102) and Shanghai Jiao Tong University School of Medicine (BXJ0807).

The authors have declared no conflict of interest.

5 References

- [1] Bingham, S., Riboli, E., Diet and cancer – the European prospective investigation into cancer and nutrition. *Nat. Rev. Cancer* 2004, 4, 206–215.
- [2] Sung, J. J., Lau, J. Y., Goh, K. L., Leung, W. K., Increasing incidence of colorectal cancer in Asia: implications for screening. *Lancet Oncol.* 2005, 6, 871–876.
- [3] Winawer, S., Faivre, J., Selby, J., Bertaro, L. *et al.*, Workgroup II: the screening process. UICC International Workshop on Facilitating Screening for Colorectal Cancer, Oslo, Norway (29 and 30 June 2002). *Ann. Oncol.* 2005, 16, 31–33.
- [4] Kim, H. J., Yu, M. H., Kim, H., Byun, J., Lee, C., Noninvasive molecular biomarkers for the detection of colorectal cancer. *Biochem Mol. Biol. Rep.* 2008, 41, 685–692.
- [5] Ramos, M., Esteva, M., Cabeza, E., Campillo, C. *et al.*, Relationship of diagnostic and therapeutic delay with survival in colorectal cancer: a review. *Eur. J. Cancer* 2007, 43, 2467–2478.
- [6] Ramos, M., Esteva, M., Cabeza, E., Llobera, J., Ruiz, A., Lack of association between diagnostic and therapeutic delay and stage of colorectal cancer. *Eur. J. Cancer* 2008, 44, 510–521.
- [7] Bembenek, A., Gretschel, S., Schlag, P. M., Sentinel lymph node biopsy for gastrointestinal cancers. *J. Surg. Oncol.* 2007, 96, 342–352.
- [8] Chau, I., Chan, S., Cunningham, D., Overview of preoperative and postoperative therapy for colorectal cancer: the European and United States perspectives. *Clin. Colorectal Cancer* 2003, 3, 19–33.
- [9] Rodriguez-Bigas, M. A., Maamoun, S., Weber, T. K., Penetrante, R. B. *et al.*, Clinical significance of colorectal cancer: metastases in lymph nodes <5 mm in size. *Ann. Surg. Oncol.* 1996, 3, 124–130.
- [10] Sarli, L., Bader, G., Iusco, D., Salvemini, C. *et al.*, Number of lymph nodes examined and prognosis of TNM stage II colorectal cancer. *Eur. J. Cancer* 2005, 41, 272–279.
- [11] Cahill, R. A., Leroy, J., Marescaux, J., Could lymphatic mapping and sentinel node biopsy provide oncological providence for local resectional techniques for colon cancer? A review of the literature. *Biomed Chromatogr. Surg.* 2008, 8, 17.
- [12] Pei, H., Zhu, H., Zeng, S., Li, Y. *et al.*, Proteome analysis and tissue microarray for profiling protein markers associated with lymph node metastasis in colorectal cancer. *J. Proteome Res.* 2007, 6, 2495–2501.
- [13] Wu, C. C., Chen, H. C., Chen, S. J., Liu, H. P. *et al.*, Identification of collapsin response mediator protein-2 as a potential marker of colorectal carcinoma by comparative

- analysis of cancer cell secretomes. *Proteomics* 2008, 8, 316–332.
- [14] Greene, F. L., Page, D. L., Fleming, I. D., Fritz, A. *et al.*, *AJCC Cancer Staging Handbook*, Springer, New York 2002.
- [15] Ilyas, M., Hao, X. P., Wilkinson, K., Tomlinson, I. P. *et al.*, Loss of Bcl-2 expression correlates with tumour recurrence in colorectal cancer. *Gut* 1998, 43, 383–387.
- [16] Rodriguez-Pineiro, A. M., Rodriguez-Berrocal, F. J., Paez de la Cadena, M., Improvements in the search for potential biomarkers by proteomics: application of principal component and discriminant analyses for two-dimensional maps evaluation. *J. Chromatogr. B Analyt. Technol. Biomed. Life Sci.* 2007, 849, 251–260.
- [17] Byvatov, E., Schneider, G., Support vector machine applications in bioinformatics. *Appl. Bioinformatics* 2003, 2, 67–77.
- [18] Vapnik, V. N., An overview of statistical learning theory. *IEEE Trans. Neural Netw.* 1999, 10, 988–999.
- [19] Hatakeyama, H., Kondo, T., Fujii, K., Nakanishi, Y. *et al.*, Protein clusters associated with carcinogenesis, histological differentiation and nodal metastasis in esophageal cancer. *Proteomics* 2006, 6, 6300–6316.
- [20] Fujii, K., Kondo, T., Yokoo, H., Yamada, T. *et al.*, Protein expression pattern distinguishes different lymphoid neoplasms. *Proteomics* 2005, 5, 4274–4286.
- [21] Seike, M., Kondo, T., Fujii, K., Okano, T. *et al.*, Proteomic signatures for histological types of lung cancer. *Proteomics* 2005, 5, 2939–2948.
- [22] Seike, M., Kondo, T., Fujii, K., Yamada, T. *et al.*, Proteomic signature of human cancer cells. *Proteomics* 2004, 4, 2776–2788.
- [23] Yokota, S., Yamamoto, Y., Shimizu, K., Momoi, H. *et al.*, Increased expression of cytosolic chaperonin CCT in human hepatocellular and colonic carcinoma. *Cell Stress Chaperones* 2001, 6, 345–350.
- [24] Coghlin, C., Carpenter, B., Dundas, S. R., Lawrie, L. C. *et al.*, Characterization and over-expression of chaperonin t-complex proteins in colorectal cancer. *J. Pathol.* 2006, 210, 351–357.
- [25] Spiess, C., Miller, E. J., McClellan, A. J., Frydman, J., Identification of the TRiC/CCT substrate binding sites uncovers the function of subunit diversity in eukaryotic chaperonins. *Mol. Cell* 2006, 24, 25–37.
- [26] Steinmann, B., Bruckner, P., Superti-Furga, A., Cyclosporin A slows collagen triple-helix formation *in vivo*: indirect evidence for a physiologic role of peptidyl-prolyl *cis-trans*-isomerase. *J. Biol. Chem.* 1991, 266, 1299–1303.
- [27] Kruse, M., Brunke, M., Escher, A., Szalay, A. A. *et al.*, Enzyme assembly after *de novo* synthesis in rabbit reticulocyte lysate involves molecular chaperones and immunophilins. *J. Biol. Chem.* 1995, 270, 2588–2594.
- [28] Rycyzyn, M. A., Clevenger, C. V., The intranuclear prolactin/cyclophilin B complex as a transcriptional inducer. *Proc. Natl. Acad. Sci. USA* 2002, 99, 6790–6795.
- [29] Fang, F., Flegler, A. J., Du, P., Lin, S., Clevenger, C. V., Expression of cyclophilin B is associated with malignant progression and regulation of genes implicated in the pathogenesis of breast cancer. *Am. J. Pathol.* 2009, 174, 297–308.
- [30] Lim, S. O., Park, S. J., Kim, W., Park, S. G. *et al.*, Proteome analysis of hepatocellular carcinoma. *Biochem. Biophys. Res. Commun.* 2002, 291, 1031–1037.
- [31] Campa, M. J., Wang, M. Z., Howard, B., Fitzgerald, M. C., Patz, E. F., jr., Protein expression profiling identifies macrophage migration inhibitory factor and cyclophilin a as potential molecular targets in non-small cell lung cancer. *Cancer Res.* 2003, 63, 1652–1656.
- [32] Yang, H., Chen, J., Yang, J., Qiao, S. *et al.*, Cyclophilin A is up-regulated in small cell lung cancer and activates ERK1/2 signal. *Biochem. Biophys. Res. Commun.* 2007, 361, 763–767.
- [33] Shen, J., Person, M. D., Zhu, J., Abbruzzese, J. L., Li, D., Protein expression profiles in pancreatic adenocarcinoma compared with normal pancreatic tissue and tissue affected by pancreatitis as detected by two-dimensional gel electrophoresis and mass spectrometry. *Cancer Res.* 2004, 64, 9018–9026.
- [34] Mikuriya, K., Kuramitsu, Y., Ryozaawa, S., Fujimoto, M. *et al.*, Expression of glycolytic enzymes is increased in pancreatic cancerous tissues as evidenced by proteomic profiling by two-dimensional electrophoresis and liquid chromatography-mass spectrometry/mass spectrometry. *Int. J. Oncol.* 2007, 30, 849–855.
- [35] Li, Z., Zhao, X., Bai, S., Wang, Z. *et al.*, Proteomics identification of cyclophilin a as a potential prognostic factor and therapeutic target in endometrial carcinoma. *Mol. Cell. Proteomics* 2008, 7, 1810–1823.
- [36] Ward, B. K., Mark, P. J., Ingram, D. M., Minchin, R. F., Ratajczak, T., Expression of the estrogen receptor-associated immunophilins, cyclophilin 40 and FKBP52, in breast cancer. *Breast Cancer Res. Treat.* 1999, 58, 267–280.
- [37] Meza-Zepeda, L. A., Forus, A., Lygren, B., Dahlberg, A. B. *et al.*, Positional cloning identifies a novel cyclophilin as a candidate amplified oncogene in 1q21. *Oncogene* 2002, 21, 2261–2269.
- [38] Leung, K. W., Tsai, C. H., Hsiao, M., Tseng, C. J. *et al.*, Pin1 overexpression is associated with poor differentiation and survival in oral squamous cell carcinoma. *Oncol. Rep.* 2009, 21, 1097–1104.
- [39] Wiegand, S., Dakic, B., Rath, A. F., Makarova, G. *et al.*, The rotamase Pin1 is up-regulated, hypophosphorylated and required for cell cycle progression in head and neck squamous cell carcinomas. *Oral. Oncol.* 2009, doi: 10.1016/j.oraloncology.2009.04.006, in press.
- [40] Choi, K. J., Piao, Y. J., Lim, M. J., Kim, J. H. *et al.*, Over-expressed cyclophilin A in cancer cells renders resistance to hypoxia- and cisplatin-induced cell death. *Cancer Res.* 2007, 67, 3654–3662.
- [41] Lu, K. P., Suizu, F., Zhou, X. Z., Finn, G. *et al.*, Targeting carcinogenesis: a role for the prolyl isomerase Pin1? *Mol. Carcinog.* 2006, 45, 397–402.